Monte Carlo calculations of correction factors for plastic phantoms in clinical photon and electron beam dosimetry

Fujio Araki,[a)]

Department of Radiological Technology, Kumamoto University School of Health Sciences, 4-24-1, Kuhonji, Kumamoto, 862-0976, Japan

Yuji Hanyu and Miyoko Fukuoka

Division of Radiation Oncology, Tokyo Women's Medical University Hospital, Japan

Kenji Matsumoto and Masahiko Okumura

Department of Central Radiology, Kinki University Hospital, Osaka, Japan

Hiroshi Oguchi

Department of Central Radiology, Shinshu University Hospital, Matsumoto, Japan

ABSTRACT

Purpose: To calculate correction factors for plastic water (PW) and plastic water diagnostic-therapy (PWDT) phantoms in clinical photon and electron beam dosimetry using the EGSnrc Monte Carlo code system.

Methods: A water-to-plastic ionization conversion factor, k_{pl}, for PW and PWDT was computed for several commonly used Farmer-type ionization chambers with different wall materials, in a range of 4-18 MV photon beams. For electron beams, a depth-scaling factor, c_{pl}, and a chamber-dependent fluence correction factor, h_{pl}, for both phantoms were also calculated in combination with NACP-02 and Roos plane-parallel ionization chambers, in a range of 4-18 MeV. The h_{pl} values for the plane-parallel chambers were evaluated from the electron fluence correction factor, ϕ_{pl}^{w}, and wall correction factors $P_{\mathrm{wall},w}$ and $P_{\mathrm{wall},pl}$ for a combination of water or plastic materials. The calculated k_{pl} and h_{pl} values were verified by comparison with the measured values.

Results and Conclusions: A set of k_{pl} values computed for the Farmer-type chambers were equal to unity within 0.5% for PW and PWDT in photon beams. The k_{pl} values also agreed within their combined uncertainty with the measured data. For electron beams, the c_{pl} values computed for PW and PWDT were from 0.998 to 1.000 and from 0.992 to 0.997, respectively, in a range of 4-18 MeV. The ϕ_{pl}^{w} values for PW and PWDT were from 0.998 to 1.001 and from 1.004 to 1.001, respectively, at a reference depth in the range of 4-18 MeV. The difference in P_{wall} between water and plastic materials for the plane-parallel chambers was 0.8% at a maximum. Finally, h_{pl} values evaluated for plastic materials were equal to unity within 0.6% for NACP-02 and Roos chambers. The h_{pl} values also agreed within their combined uncertainty with the measured data. The absorbed dose to water from ionization chamber measurements in PW and PWDT plastic materials corresponds to that in water within 1%. Both phantoms can thus be used as a substitute for water for photon and electron dosimetry.

Key words: water-to-plastic ionization conversion factor, fluence correction factor, wall correction factor, chamber-dependent fluence correction factor, Monte Carlo calculations

I. INTRODUCTION

Recent standard dosimetry protocols[1-4] recommend that a water phantom be used in the calibration of high-energy photon and electron beam treatment units. It is recognized, however, that this may be time-consuming and that the use of a plastic phantom may be more convenient for routine use such as quality assurance measurements due to simplicity, robustness, and positioning accuracy and reproducibility. IAEA TRS-398, JSMP-2002 and IPEM-2003 protocols allow thus the use of plastic phantoms, especially for the calibration of low-energy electron beams with beam qualities R_{50} < 4 g/cm^2. Also, for the determination of an absorbed dose at the reference point for low-energy, the preferred detector is a plane-parallel ionization chamber because of good depth resolution.

The main problem with plastic phantoms is that the dose measured must be converted to the absorbed dose to water at a reference point situated at an equivalent depth in water. For photon beams, Seuntjens *et al*.[5] presented methods to determine the absorbed dose to water from ionization chamber measurements in a plastic phantom within the context of absorbed dose calibration protocols. In their paper, the ratio of the electrometer reading in the water phantom to that in the plastic phantom, that is, a water-to-plastic ionization conversion factor, k_{pl}, is evaluated from Monte Carlo methods at a water-equivalent reference depth. The water-equivalent depth in plastic is scaled from the relative electron density to water, which corresponds to the depth-scaling factor, c_{pl}.

Corrections for electron beam dosimetry are required for differences in stopping power and scattering power. The water-to-plastic ionization conversion factor for electron beams is known as a chamber-dependent fluence correction factor, h_{pl}.[6-9] h_{pl} can be computed from the electron fluence correction factor, ϕ_{pl}^{w}, and the wall correction factor, P_{wall}, of the ionization chamber used,[8,9] which accounts for the non-phantom equivalence of the chamber wall material. ϕ_{pl}^{w} is the ratio of the electron fluence in the water phantom to that in the plastic phantom and accounts for the difference in the electron fluence in the two phantoms at the same water-equivalent depth. h_{pl} is equal to ϕ_{pl}^{w} when P_{wall} in water and plastic is the same. The electron spectra in the two phantom materials are also identical in shape at the two positions of water-equivalent depth.[7,9]

So far there have been many studies on calculated ϕ_{pl}^{w} values and measured h_{pl} values for various plastic phantoms in electron beam dosimetry,[6-16] and the measured h_{pl} values for several plastic phantoms are summarized in the IAEA TRS-398 code of practice. However, there have been only few studies[9] on calculated h_{pl} values that considered two wall correction factors, $P_{\mathrm{wall},w}$ and $P_{\mathrm{wall},pl,}$ for a combination of water or plastic phantoms and wall materials of plane-parallel chambers because it is difficult to obtain wall correction factors experimentally, especially for plane-parallel chambers. In photon beam dosimetry, the dose ratio of plastic to water was obtained from ionization chamber measurements in several plastic phantom materials by Tello *et al.*[10] Seuntjens *et al.*[5] presented the validity of k_{pl} calculated with Monte Carlo methods from a comparison by ionization chamber measurements for solid water RMI-457 and PMMA phantoms.

This study has evaluated the correction factors for plastic water (PW)[16] and Plastic Water Diagnostic-Therapy (PWDT)[17] epoxy-resin materials manufactured by Computerized Imaging Reference Systems Inc. (CIRS, Norfolk, VA). PW and PWDT phantoms are made to match attenuation and absorption properties to water over photon energy of 150 keV-100 MeV and 50 keV-25 MeV, respectively. PWDT can then be used at both diagnostic and therapeutic energies. Since their electron densities [el/cm^3] and effective atomic numbers are very close to water compared to other plastic phantom materials, both phantoms can also be used for electron beam dosimetry. Tello *et al.*[10] presented that k_{pl} and h_{pl} values of PW for photon and electron beams are equal to unity within approximately 0.5% from measurements using a Farmer-type chamber. The h_{pl} value of PW is adopted in the IAEA TRS-398 code of practice. The PW material used in this study is slightly different from the previous one in terms of elemental composition in fraction by weight and nominal mass density.[16] In this study, the k_{pl} values for PW and PWDT were computed by Monte Carlo methods for several commonly used Farmer-type ionization chambers with different wall materials, in the range of 4-18 MV photon beams. The c_{pl} and h_{pl} values for plastic phantom materials were also calculated in combination with an NACP-02 chamber or a Roos chamber, in a range of 4-18 MeV electron beams. The calculated k_{pl} and h_{pl} values were verified by comparison with the measured values.

II. THEORY

II.A. Water-to-plastic ionization conversion factor, k_{pl}, for photon beams

k_{pl} at a water-equivalent reference depth in plastic phantoms for photon beams can be calculated according to the Spencer-Attix cavity theory:[5]

$$k_{pl} = \frac{D_w(d_{\text{ref}}) / (\bar{L}/\rho)^{w}_{\text{air}}}{D_{pl}(d_{\text{eq}}) / (\bar{L}/\rho)^{pl}_{\text{air}}} \cdot \frac{P_{Q,pl}}{P_{Q,w}}, \qquad (1)$$

where D_w and D_{pl} are the doses to water and plastic, respectively, d_{ref} and d_{eq} are the reference depth in water and the water-equivalent reference depth in plastic, respectively, $(\bar{L}/\rho)^{pl}_{\text{air}}$ and $(\bar{L}/\rho)^{w}_{\text{air}}$ are the average restricted collision stopping-power ratios of plastic to air and water to air, respectively, and $P_{Q,pl}$ and $P_{Q,w}$ are the overall perturbation correction factors for the cylindrical ionization chamber in plastic and water, respectively. D_w, D_{pl}, $(\bar{L}/\rho)^{w}_{\text{air}}$, and $(\bar{L}/\rho)^{pl}_{\text{air}}$ can be calculated directly using Monte Carlo methods. In this study P_Q for the cylindrical ionization chambers considers only wall correction factors $P_{\text{wall},w}$ and $P_{\text{wall},pl}$ in water and plastic. The replacement and central electrode corrections for PW and PWDT phantoms are assumed to be the same as those for water and they are canceled out in Eq. (1).

Experimentally, k_{pl} can be measured as a ratio of ionization chamber readings M_w and M_{pl} in the water phantom at depth d_{ref} and the plastic phantom at depth d_{eq}, respectively,

$$k_{pl} = \frac{M_w(d_{\text{ref}})}{M_{pl}(d_{\text{eq}})}. \qquad (2)$$

Typically, d_{ref} in water for photon beams is 10 cm, resulting in an equivalent depth $d_{\text{eq}}=d_{\text{ref}}/\rho_e(pl)$ for the plastic phantom, where $\rho_e(pl)$ is the relative electron density of plastic to water.

II.B. Depth-scaling factor, c_{pl}, for electron beams

c_{pl} for a plastic phantom in electron beams in the IAEA TRS-398 code of practice[2] is given by

$$c_{pl} = \frac{I_{50,w}}{I_{50,pl}}, \qquad (3)$$

where $I_{50,w}$ and $I_{50,pl}$ are the depths (in cm) at which the ionization curve falls to one-half of its maximum value in water and plastic, respectively. Strictly, c_{pl} factors are applied only for depth-dose distributions and their use in scaling depth-ionization distributions is an approximation, but the c_{pl} values obtained from both methods are almost the same and thus

the use of I_{50} is practical since it can be obtained experimentally. The depth in water, d, is related to the depth in plastic, d_{eq}, by c_{pl}:

$$d = d_{\mathrm{eq}} c_{pl}. \qquad (4)$$

The scaled (water-equivalent) reference depth in plastic can be calculated from Eq. (4).

II.C. Correction factors, ϕ_{pl}^{w} and h_{pl}, for electron beams

ϕ_{pl}^{w} at a water-equivalent depth in plastic phantoms is calculated according to Spencer-Attix cavity theory:[7,9]

$$\phi_{pl}^{w} = \frac{D_w(d)/(\bar{L}/\rho)_{\mathrm{air}}^{w}}{D_{pl}(d_{\mathrm{eq}})/(\bar{L}/\rho)_{\mathrm{air}}^{pl}}. \qquad (5)$$

where D_w and D_{pl} are the doses to water and plastic, respectively. D_w, D_{pl}, $(\bar{L}/\rho)_{\mathrm{air}}^{w}$, and $(\bar{L}/\rho)_{\mathrm{air}}^{pl}$ are calculated with Monte Carlo methods in this paper.

In the IAEA TRS-398 code of practice[2], h_{pl} is defined as the ratio of the electrometer reading, M_w, at d_{ref} in water and equivalent reading, M_{pl}, at d_{eq} in plastic by

$$h_{pl} = \frac{M_w(d_{\mathrm{ref}})}{M_{pl}(d_{\mathrm{eq}})}. \qquad (6)$$

h_{pl} is given as the fluence-scaling factor in the IAEA TRS-398 code of practice but the present study uses the chamber-dependent fluence correction factor. In Eq. (6) h_{pl} is generally obtained from cross measurements at the reference depth in water and plastic as well as Eq. (2) for photon beams. In the calculations, h_{pl} can be expressed as follows:[8,9]

$$h_{pl} = \phi_{pl}^{w} \frac{(P_{\mathrm{fl}}P_{\mathrm{wall}})_{pl}}{(P_{\mathrm{fl}}P_{\mathrm{wall}})_{w}}. \qquad (7)$$

P_{fl} in water and plastic phantoms is canceled in Eq. (7) because the reference depth in plastic is scaled to that in water, which means the fluence spectra are the same and so P_{fl} values are the same. The relationship of h_{pl} and ϕ_{pl}^{w} is thus given by

$$h_{pl} = \phi_{pl}^{w} \frac{P_{\mathrm{wall},pl}}{P_{\mathrm{wall},w}}. \qquad (8)$$

P_{wall} for plane-parallel chambers in water and plastic is calculated using Monte Carlo methods. Equation (8) is equivalent to Eq. (1) for photon beams.

III. METHODS AND MATERIALS

III.A. Plastic phantoms

Plastic water and plastic water DT materials (CIRS, Norfolk, VA) were used as water-equivalent plastic phantoms. The elemental composition in fraction by weight, mass density, ρ [g/cm^3], electron densities, ρ_e*[el/g] and ρ_e [el/cm^3], for water and the plastic phantoms, the relative electron densities of plastic to water, ρ_e*(pl) and ρ_e (pl), and the effective atomic number, $\bar{Z}$,[18] are presented in Tables I and II. ρ_e*[el/g] is calculated by

$$\rho_e^* = \sum_i \frac{N_A w_i Z_i}{A_i}, \qquad (9)$$

where N_A is Avogadro's number, w_i is the fraction by weight of element i, and Z_i and A_i are the atomic number and atomic weight of i, respectively. ρ_e [el/cm^3] is given by

$$\rho_e = \rho_e^* \times \rho . \qquad (10)$$

III.B. Monte Carlo simulations

The EGSnrc[19]/BEAMnrc code[20,21] was used to simulate photon and electron beams emerging from a Varian Clinac linear accelerator (Varian Oncology Systems, Palo Alto, CA). The accuracy of beam modeling for Monte Carlo simulations was verified by comparing with measured dose distributions for photon and electron beams. The phantoms were set at a source-to-surface distance (SSD) of 100 cm, and a field size at the phantom surface was 10 × 10 cm^2 for photon beams and 15 × 15 cm^2 for electron beams. The position, energy, angle, charge and weight of particles crossing the phase space plane were scored in phase space files. The phase space data were taken below the secondary collimator for photon beams and the applicator for electron beams. The dose distributions for each beam in water and plastic phantoms were calculated with the EGSnrc/DOSXYZnrc code[22] using the phase space data as input. The parameters used for simulations were: AE=0.521 MeV, ECUT=0.700 MeV, AP=PCUT=0.01 MeV.

The incident electron energy was adjusted to agree within 2% between Monte Carlo calculated and measured dose distributions (central axis depth-dose curve and off-axis dose profile at a depth of dose maximum) in a water phantom. Table III presents the characteristics of photon and electron beams from the Varian Clinac linear accelerators used in this study.

III.B.1. k_{pl} for photon beams

The absorbed doses, D_w and D_{pl}, at scaled depths in water and plastic phantoms were evaluated with Monte Carlo methods to calculate k_{pl} using Eq. (1). The stopping-power ratios were also calculated for application of cavity theory in both water and the plastic phantoms. P_{wall} for the cylindrical ionization chamber in water and plastic phantoms was evaluated from the stopping power ratios combined with the average mass-energy absorption coefficient ratios according to Eq. (62) in the IAEA TRS-277 code of practice.[23] The mass-energy absorption coefficient ratio of phantom material, "*m*", to chamber wall material, "wall", for any spectrum is calculated by the ratio of collision kerma for both materials:[24]

$$\left(\frac{\bar{\mu}_{\mathrm{en}}}{\rho}\right)_{\mathrm{wall}}^{m} = \frac{\sum_i E_i \Phi(E_i)[\mu_{\mathrm{en}}(E_i)/\rho]_m}{\sum_i E_i \Phi(E_i)[\mu_{\mathrm{en}}(E_i)/\rho]_{\mathrm{wall}}} \qquad (11)$$

where E_i is the photon energy, and $\Phi(E_i)$ is the photon fluence spectrum. $\mu_{\mathrm{en}}(E_i)/\rho$ for each photon energy is obtained from the data of Seltzer and Hubbell.[25] The photon fluence spectrum and stopping-power ratios were calculated from the phase space data at a water-equivalent reference depth using EGSnrc user-codes FLURZnrc[26] and SPRRZnrc,[26] respectively. ECUT and PCUT were 0.521 MeV and 0.01 MeV, respectively.

III.B.2. c_{pl} and ϕ_{pl}^{w} for electron beams

A depth-scaling factor for PW and PWDT was evaluated with Monte Carlo methods. First, the central axis depth-dose curves for water and plastic phantoms calculated in Sec. III.B were transferred to depth-ionization curves or depth-fluence curves by dividing with respective calculated Spencer-Attix stopping power ratios, in order to determine $I_{50,w}$ and $I_{50,pl}$ for each electron beam. The c_{pl} values for plastic phantoms were then obtained from Eq. (3). Stopping-power ratios were calculated from the phase space data using the EGSnrc/SPRRZnrc code.

The ratio of electron fluence between water and plastic phantoms was obtained from the ratio of depth-ionization curves of water to plastic using Eq. (5). The ϕ_{pl}^{w} values were calculated as a function of a water-equivalent depth in each electron beam.

III.B.3. P_{wall} and h_{pl} for electron beams

Wall correction factors at the water-equivalent reference depth for a combination of water or plastic phantoms and wall materials of NACP-02 and Roos chambers were calculated using Monte Carlo methods described in previous papers.[9,27,28] For the P_{wall} calculation, the electron spectra obtained from the phase space data were used as the electron source. This is because a huge phase space data set is needed to compute P_{wall} with a statistical accuracy less than 0.2%. Also, the difference of the contaminant photons in P_{wall} calculation between the phase space data and the electron spectra is not significant since P_{wall} is obtained as the ratio of two doses. The ratio of the dose to the sensitive volume in the air cavity for a chamber wall composed entirely of water or plastic to that for a real chamber geometry was computed with the EGSnrc/CAVRZnrc code.[26]

Finally, the chamber-dependent fluence correction factor for plastic materials at the water-equivalent reference depth was obtained from Eq. (8) using ϕ_{pl}^{w} and P_{wall} correction factors for water to plastic.

III.C. Measurements of k_{pl} and h_{pl}

The k_{pl} values for photon beams were cross measured with a PTW 30001 Farmer-type chamber at the reference depth in water and plastic phantoms according to Eq. (2). The point of measurement for the chamber was taken to be a center of the air cavity. The h_{pl} values for electron beams were also cross measured with NACP-02 and Roos chambers at the reference depth in water and plastic phantoms according to Eq. (6). The point of measurement for the plane-parallel chambers was at the front face of the air cavity. Both phantoms were irradiated with a 10 × 10 cm^2 field at a source-axis distance (SAD) of 100 cm for photons and a 15 × 15 cm^2 field at an SSD of 100 cm for electrons from a Varian Clinac linear accelerator. The measured k_{pl} and h_{pl} values were compared with those calculated.

IV. RESULTS AND DISCUSSION

IV.A. Determination of k_{pl} for photon beams

The cylindrical ionization chambers used in this study were the Farmer-type of PTW 30001 and 30013 (PMMA wall), PTW 30002 and 30004 (Carbon wall), and Exradin A12 (C552 wall). The geometries and materials for the chambers are presented in detail in Table III of the IAEA TRS-398 code of practice. The water-equivalent reference depths for PW and PWDT

phantoms were taken at the same depth as water of 10 cm since the relative electron densities ρ_e (pl) are 1.000 and 1.003, respectively, as shown in Table II. Table IV summarizes the mass-energy absorption coefficient ratios of phantom materials (water, PW, and PWDT) to chamber wall materials (C552, Carbon, and PMMA), as a function of beam quality expressed in TPR_{10}^{20} and $\%\mathrm{dd}(10)_x$. Similarly, the stopping-power ratios of phantom materials to air and chamber wall materials to air are summarized in Table V.

Ratios of wall correction factors for the Farmer-type chambers in PW and PWDT relative to water were calculated using the mass-energy absorption coefficient ratios and stopping-power ratios and the results are summarized in Table VI. The ratio $(P_{\mathrm{wall}})_{pl}^{w}$ is close to unity since the plastic materials have an electron density (el/cm^3) similar to water. Table VII summarizes the k_{pl} values calculated for the Farmer-type chambers in PW and PWDT from Eq. (1). The statistical uncertainty (1σ) of k_{pl} values is estimated to be 0.6%-0.7% considering the 0.5% uncertainty of $(P_{\mathrm{wall}})_{w}^{pl}$ [2] in Eq. (1). The k_{pl} values for the Farmer-type chambers in both phantoms are from 0.995 to 1.001, in a range of 4-18 MV, and are equal to unity within 0.5%. The results of PW are similar to the values for the previous PW model measured by Tello *et al.*[10] The PWDT values also agree within the uncertainties with those measured by Ramaseshan *et al.*[17] Figures 1(a) and 1(b) present a comparison of calculated and measured k_{pl} values for the PTW 30001 chamber. Measurements were performed with PW and PWDT for 4, 6, and 10 MV photon beams from Varian Clinac linear accelerators. The uncertainties of k_{pl} measurements are estimated as 0.3% (1σ) from the uncertainties of the chamber positioning and readings in water and plastic. The calculated k_{pl} values for both materials agree within their combined uncertainty (1σ=0.7%) with the measured data.

IV.B. Correction factors for electron beams

IV.B.1 Calculation of c_{pl}, ϕ_{pl}^{w}, and P_{wall}

Figure 2 presents Monte Carlo calculated depth-scaling factors for PW and PWDT phantom materials as a function of I_{50} in clinical electron beams. The scaling factors for PW and PWDT are 0.998 to 1.000 and 0.992 to 0.997, respectively, in the range of nominal energies from 4 to 18 MeV. In other words, the two phantom materials show almost the same depth-ionization curves or depth-fluence curves as water. The results are similar to the value (c_{pl}=0.991) for the previous PW model calculated by Fernandez-Varea *et al.*[29]

Figures 3(a)-3(f) present electron fluence correction factors calculated according to Eq. (5) for realistic electron beams from Varian Clinac linear accelerators. The ϕ_{pl}^{w} curves for PW and PWDT phantoms are shown as a function of water-equivalent depth in the range of nominal energies from 4 to 18 MeV. The ratio ϕ_{pl}^{w} depends on the depth-ionization curves or depth-fluence curves of water and plastic phantoms. The electron fluence for both plastic materials agrees with that of water within ±0.5% up to around R_{50} at all the electron energies.

The ϕ_{pl}^{w} value at the reference depth is the most important in the clinical dose calibration. Figure 4 shows calculated fluence correction factors as a function of R_{50} at the water-equivalent reference depth for plastic phantoms. The statistical uncertainties of ϕ_{pl}^{w} values at the reference depth are within 0.3%. The ϕ_{pl}^{w} values for PW are almost constant from 0.998 at 4 MeV to 1.001 at 18 MeV, and similarly are from 1.004 to 1.001 for PWDT. The ϕ_{pl}^{w} values for both phantom materials are almost the same due to their similar composition (Table I), and they are very close to unity compared to those of water-equivalent plastic materials reported by previous papers.[7,9,13]

Figures 5(a) to 5(b) show P_{wall} values calculated as a function of R_{50} for NACP-02 and Roos plane-parallel chambers. The nominal electron energies range from 4 to 18 MeV, and the values are calculated at the reference depth in water and the water-equivalent depth in plastic phantoms. The statistical uncertainties of P_{wall} for NACP-02 and Roos chambers are 0.2% and 0.14%, respectively. The size of $P_{\mathrm{wall},w}$ corrections in water for the NACP-02 and Roos chambers are in reasonable agreement with those estimated using the EGSnrc Monte Carlo codes by previous papers.[9,27,28] The differences in P_{wall} between water and plastic materials for the plane-parallel chambers are 0.8% at a maximum. $P_{\mathrm{wall},pl}$ in both phantoms also shows energy dependence similar to that in water. This is because their effective atomic number is similar to that of water as shown in Table I. The main attribution for the wall correction of the plane-parallel chambers arises from the difference in the backscatter in the chamber wall material and the phantom material.[30-32]

IV.B.2. Determination of h_{pl}

Table VIII presents h_{pl} values calculated using Eq. (8) at the water-equivalent reference depth

for the combination of plastic phantoms and plane-parallel chambers. The ϕ_{pl}^{w}, $P_{\mathrm{wall},w}$, and $P_{\mathrm{wall},pl}$ values in Eq. (8) are obtained from relative calculated values for each phantom material in Figs. 4 and 5. The uncertainties of h_{pl} values evaluated from each calculated correction factor are 0.4% and 0.3% for NACP-02 and Roos chambers, respectively. For the combination of the NACP-02 chamber and PW, h_{pl} values vary from 1.006 to 0.998, in the range of 4-18 MeV. The h_{pl} values of PW for the Roos chamber are 0.998-1.003, almost independent of electron energy. The h_{pl} values for both chambers in PW are close to the ϕ_{pl}^{w} values since the wall correction factor in PW almost corresponds to that in water. The results are then similar to the values for the previous PW model measured with the Farmer-type chamber by Tello *et al.*[12] The calculated h_{pl} values of PWDT are 1.006-0.997 for the NACP-02 chamber and 0.998-1.005 for the Roos chamber, in the range of 4-18 MeV. The h_{pl} values of PWDT for each chamber are consistent with those of PW within the statistical uncertainties.

The comparison of calculated and measured h_{pl} values for the NACP-02 chamber is presented in Figs. 6(a) and 6(b). Measurements were performed using PW and PWDT at nominal energies of 6, 9, and 18 MeV from a Varian Clinac linear accelerator. The uncertainties of h_{pl} measurements are estimated from the positioning uncertainty of the chamber and the standard deviation (1σ=0.1%) of the chamber readings at the reference depth in water and plastic phantoms. The positioning uncertainty was 0.5 mm and this corresponds to the reading error of 0.1%-0.2%. Thus, the h_{pl} values are estimated to have uncertainties of 0.3% from the ionization ratios in water and plastic. The calculated h_{pl} values in both materials agree within their combined uncertainty (1σ=0.5%) with the measured data.

V. CONCLUSIONS

This paper has investigated correction factors for the use of PW and PWDT plastic phantoms in clinical photon and electron dosimetry using the EGSnrc Monte Carlo code system. The k_{pl} values for several commonly used Farmer-type chambers were equal to unity within 0.5% for both plastic phantoms in the range of 4-18 MV photon beams. The calculated k_{pl} values agreed within their combined uncertainty with the measured data. The c_{pl} values for electron beams were from 0.998 to 1.000 for PW and from 0.992 to 0.997 for PWDT, in the range of nominal energies from 4 to 18 MeV and were almost independent of electron energy. The ϕ_{pl}^{w}

values at the reference depth were equal to unity within 0.4% for the both phantoms, and they are very close to unity compared to those of water-equivalent plastic materials reported by previous papers. The wall correction factors for NACP-02 and Roos chambers in both phantoms almost agreed with those in water and the difference was 0.8% at a maximum. The h_{pl} values evaluated for the plastic phantoms were equal to unity within 0.6% for NACP-02 and Roos chambers. The h_{pl} values also agreed within their combined uncertainty with the measured data. The absorbed dose to water from ionization chamber measurements in PW and PWDT plastic materials corresponds to that in water within 1%. Both phantoms can thus be used as a substitute for water for photon and electron dosimetry.

ACKNOWLEDGMENTS

The authors thank Varian Oncology Systems for providing detailed treatment head designs to simulate Varian Clinac accelerators. The authors also thank the Euro Medi Tech Co. in Japan for providing PW and PWDT phantoms. This study was partially supported by a Grant in-Aid for Scientific Research (C), 19591460.

REFERENCES

[a)]Corresponding author. Electronic mail: f_araki@kumamoto-u.ac.jp

[1]P. R. Almond, P. J. Biggs, B. M. Coursey, W. F. Hanson, M. S. Huq, R. Nath, and D. W. O. Rogers, “AAPM’s TG-51 protocol for clinical reference dosimetry of high-energy photon and electron beams,” Med. Phys. **26**, 1847-1870 (1999).

[2]IAEA, “Absorbed dose determination in external beam radiotherapy: An international code of practice for dosimetry based on standards for absorbed dose to water,” Technical Report Series No. 398, (IAEA, Vienna, 2000).

[3]JSMP: Japanese Society of Medical Physics, “The standard dosimetry of absorbed dose in external beam radiotherapy,” Tsusho-sangyo-kenkyusya, Tokyo, 2002 (in Japanese).

[4]IPEM, “The IPEM code of practice for electron dosimetry for radiotherapy beams of initial energy from 4 to 25 MeV based on an absorbed dose to water calibration,” Phys. Med. Biol. **48**, 2929-2970 (2003).

[5]J. Seuntjents, M. Olivares, M. Evans, and E. Podgorsak, “Absorbed dose to water reference dosimetry using solid phantoms in the context of absorbed-dose protocols,” Med. Phys. **32**, 2945-2953 (2005).

[6]D. I. Thwaites, “Measurements of ionization in water, polystyrene and a ‘solid water’ phantom material for electron beams,” Phys. Med. Biol. **30**, 41-53 (1985).

[7]G. X. Ding, D. W. O. Rogers, J. E. Cygler, and T. R. Mackie, “Electron fluence correction factors for conversion of dose in plastic to dose in water,” Med. Phys. **24**, 161-176 (1997).

[8]B. Nilsson, A. Montelius, P. Andreo, and J. Johansson, “Correction factors for parallel-plate chambers used in plastic phantoms in electron dosimetry,” Phys. Med. Biol. **42**, 2101-2118 (1997).

[9]F. Araki, “Monte Carlo study of correction factors for the use of plastic phantoms in clinical electron beams,” Med. Phys. **34**, 4368-4377 (2007).

[10]V. M. Tello, R. C. Tailor, and W. F. Hanson, “How water equivalent are water-equivalent solid materials for output calibration of photon and electron beams?,” Med. Phys. **22**, 1177-1189 (1995).

[11]B. Nilsson, A. Montelius, and P. Andreo, “Wall effect in plane-parallel ionization chambers,” Phys. Med. Biol. **41**, 609-623 (1996).

[12]A. Nisbet and D. I. Thwaites, “An evaluation of epoxy resin phantom materials for electron dosimetry,” Phy. Med. Biol. **43**, 1523-1528 (1998).

[13]E. A. Siegbahn, B. Nilsson, J. M. Fernandez-Varea, and P. Andreo, “Calculations of electron fluence correction factors using the Monte Carlo code PENELOPE,” Phys. Med. Biol. **48**, 1263-1275 (2003).

[14]M. R. McEwen and A. R. DuSautoy, “Characterization of water-equivalent material WTe for use in electron beam dosimetry,” Phys. Med. Biol. **48**, 1885-1893, (2003).

[15]M. R. McEwen and D. Niven, “Characterization of the phantom material Virtual Water™ in high-energy photon and electron beams,” Med. Phys. **33**, 876-887 (2006).

[16]P. Carrasco, N. Jornet, M. A. Duch, V. Panettieri, L. Weber, T. Eudaldo, M. Ginjaume, and M. Ribas, “Comparison of dose calculation algorithms in slab phantoms with cortical bone equivalent heterogeneities, Med. Phys. 34, 3323-333 (2007).

[17]R. Ramaseshan, K. Kohli, F. Cao, and R. Heaton, “Dosimetric evaluation of Plastic Water Diagnostic Therapy, J. Appl. Clinic. Med. Phys. 9, 98-111 (2008).

[18]ICRU, “Radiation dosimetry: Electron beams with energies between 1 and 50 MeV, Report 35, (ICRU, Bethesda, MD, 1984)

[19]I. Kawrakow and D.W.O. Rogers, “The EGSnrc code system: Monte Carlo Simulation of Electron and Photon Transport,” National Research Council of Canada Report PIRS-701 (2002).

[20]D. W. O. Rogers, B. A. Faddegon, G. X. Ding, C. M. Ma, J. We, and T. R. Mackie, “BEAM: a Monte Carlo code to simulate radiotherapy treatment units,” Med. Phys. **22**, 503-524 (1995).

[21]D.W. O. Rogers, C. Ma, G.. X. Ding, B. R. Walters, D. Sheikh-Bagheri, and G. G.. Zhang, “BEAMnrc user’s manual,” National Research Council of Canada Report PIRS-509 (a) Rev F (2001).

[22]C. M. Ma, D. W. O. Rogers and B. R. Walters, “DOSXYZnrc user’s manual,” National Research Council of Canada Report PIRS-509 (b) Rev F (2001).

[23]IAEA, “Absorbed dose determination in photon and electron beams: An international

code of practice," Technical Report Series No. 277, 2nd ed. (IAEA, Vienna, 1997).

[24]A. K. Ho and B. R. Paliwai, "Stopping-power and mass energy-absorption coefficient ratios for solid water", Med. Phys. **13**, 403-404 (1986).

[25]S. M. Seltzer and J. H. Hubbell, "Tables and graphs of photon mass attenuation coefficients and mass energy-absorption coefficients for photon energies 1 keV to 20 MeV for elements Z = 1 to 92," the x-ray attenuation and absorption for materials of dosimetric interest database, (NIST, 1996).

[26]D.W. O. Rogers, I. Kawrakow, J. P. Seuntjens, B. R. Walters, and E. Mainegra-Hing, "NRC User Codes for EGSnrc," National Research Council of Canada Report PIRS-702 Rev B (2005).

[27]L. A. Buckley and D. W. O. Rogers, "Wall correction factors, P_{wall}, for parallel-plate ionization chambers," Med. Phys. **33**, 1788-1796 (2006).

[28]F. Araki, "Monte Carlo calculations of correction factors for plane-parallel ionization chambers in clinical electron dosimetry," Med. Phys. **35**, 4033-4040 (2008).

[29]J. M. Fernandez-Varea, P. Andreo, and T Tabata, "Detour factors in water and plastic phantoms and their use for range and depth scaling in electron-beam dosimetry," Phys. Med. Biol. **41**, 1119-1139 (1996).

[30]M. A. Hunt, G. J. Kutcher, and A. Buffa, "Electron backscatter corrections for parallel-plate chambers," Med. Phys. **15**, 96-103 (1988).

[31]S. C. Klevenhagen, "Implication of electron backscattering for electron dosimetry," Phys. Med. Phys. **36**, 1013-1018 (1991).

[32]M. McEwen, H. Palmans, and A. Williams, "An empirical method for the determination of wall perturbation factors for parallel-plate chambers in high-energy electron beams,"

Phys. Med. Biol. 51, 5167–5181 (2006).

Table Captions

Table I. The elemental composition in fraction by weight of phantom materials used in the Monte Carlo calculations. The data for plastic materials are provided by CIRS Inc.

Element	Water	PW	PWDT
H	0.1119	0.0779	0.0740
B			0.0226
C		0.5982	0.4670
N		0.0178	0.0156
O	0.8881	0.2357	0.3352
Mg			0.0688
Al			0.0140
Cl		0.0023	0.0024
Ca		0.0676	
$\overline{Z}^{a}$	6.60	6.64	6.43

[a] $\overline{Z}$ is calculated from the ICRU report 35 (Ref. 18).

Table II. Mass density, ρ [g/cm^3], and electron densities, ρ_e*[el/g] and ρ_e [el/cm^3], for phantom materials, and the relative electron densities of plastic to water, ρ_e*(pl) and ρ_e(pl). Mass densities for plastic materials are provided by CIRS Inc.

Density	Water	PW	PWDT
ρ [g/cm^3]	0.998[a]	1.030	1.039
ρ_e*[el/g][b]	3.343×10^{23}	3.238×10^{23}	3.218×10^{23}
ρ_e*(pl)	1.000	0.969	0.963
ρ_e [el/cm^3][c]	3.335×10^{23}	3.335×10^{23}	3.344×10^{23}
ρ_e(pl)	1.000	1.000	1.003

[a]Mass density for pure water at 22.0 ℃.
[b]ρ_e* is calculated from Eq. (9) in text.
[c]$\rho_e=\rho_e^*\times\rho$

Table III. Characteristics of clinical photon and electron beams from the Varian Clinac linear accelerators. The reference depth, d_{ref}, is obtained from $0.6R_{50}$-0.1 (cm).

Photon beams		
$E_{nominal}$ (MV)	%dd(10)$_x$	TPR_{10}^{20}
4	61.8	0.615
6	66.3	0.669
10	73.3	0.737
18	80.9	0.779
Electron beams		
$E_{nominal}$ (MeV)	R_{50} (cm)	d_{ref} (cm)
4	1.31	0.69
6	2.37	1.32
9	3.59	2.05
12	5.06	2.94
15	6.27	3.66
18	7.60	4.46

530

535

Table IV. Average mass-energy absorption coefficient ratios of phantom material to chamber wall materials as a function of beam quality expressed in TPR_{10}^{20} and $\%dd(10)_x$. Phantom materials: water (*w*), PW, and PWDT. Wall materials: C552, Carbon, and PMMA.

540

TPR_{10}^{20}	$\%dd(10)_x$	$(\bar{\mu}_{en}/\rho)_{wall}^{w}$	$(\bar{\mu}_{en}/\rho)_{wall}^{PW}$	$(\bar{\mu}_{en}/\rho)_{wall}^{PWDT}$
		Wall=C552		
0.615	61.8	1.110	1.082	1.069
0.669	66.3	1.109	1.078	1.067
0.737	73.3	1.105	1.072	1.062
0.779	80.9	1.099	1.065	1.055
		Wall=Carbon		
0.615	61.8	1.114	1.087	1.073
0.669	66.3	1.114	1.083	1.073
0.737	73.3	1.118	1.084	1.075
0.779	80.9	1.124	1.089	1.079
		Wall=PMMA		
0.615	61.8	1.031	1.006	0.993
0.669	66.3	1.032	1.004	0.994
0.737	73.3	1.037	1.006	0.997
0.779	80.9	1.045	1.012	1.003

Table V. Average restricted collision stopping-power ratios of medium to air as a function of beam quality expressed in TPR_{10}^{20} and $\%dd(10)_x$. Medium: Water, PW, PWDT, C552, Carbon, and PMMA.

TPR_{10}^{20}	$\%dd(10)_x$	$(\bar{L}/\rho)_{air}^{med}$					
		Water	PW	PWDT	C552	Carbon	PMMA
0.615	61.8	1.1278	1.0927	1.0814	0.9903	0.9963	1.0957
0.669	66.3	1.1208	1.0852	1.0746	0.9836	0.9876	1.0878
0.737	73.3	1.1056	1.0703	1.0606	0.9700	0.9722	1.0722
0.779	80.9	1.0894	1.0546	1.0454	0.9558	0.9576	1.0556

Table VI. Ratios of wall correction factors for the Farmer-type chambers in PW and PWDT relative to water as a function of beam quality expressed in TPR_{10}^{20} and $\%dd(10)_x$. Chamber wall materials: PMMA, Carbon, and C552.

	TPR_{10}^{20}	0.615	0.669	0.737	0.779
Chamber	$\%dd(10)_x$	61.8	66.3	73.3	80.9
$(P_{wall})_w^{PW}$					
PTW 30001 (PMMA)		1.002	1.000	0.999	0.999
PTW 30013 (PMMA)		1.002	1.001	1.000	1.000
PTW 30002 & 30004 (Carbon)		1.002	1.001	0.999	0.999
Exradin A12 (C552)		1.003	1.001	1.000	1.000
$(P_{wall})_w^{PWDT}$					
PTW 30001 (PMMA)		1.001	1.000	0.999	0.998
PTW 30013 (PMMA)		1.002	1.001	1.000	1.000
PTW 30002 & 30004 (Carbon)		1.002	1.001	0.999	0.999
Exradin A12 (C552)		1.002	1.001	1.000	1.000

Table VII. Water-to-plastic ionization conversion factors k_{pl} for the Farmer-type chambers in PW and PWDT phantoms as a function of beam quality expressed in TPR_{10}^{20} and $\%dd(10)_x$.

	TPR_{10}^{20}	0.615	0.669	0.737	0.779
Chamber	$\%dd(10)_x$	61.8	66.3	73.3	80.9
PW					
PTW 30001		0.996	0.997	0.998	1.000
PTW 30013		0.997	0.998	0.999	1.001
PTW 30002 & 30004		0.997	0.998	0.998	1.000
Exradin A12		0.998	0.998	0.999	1.001
PWDT					
PTW 30001		0.995	0.997	0.999	0.999
PTW 30013		0.996	0.998	1.000	1.001
PTW 30002 & 30004		0.996	0.998	0.999	1.000
Exradin A12		0.996	0.998	1.000	1.001

Table VIII. Calculated chamber-dependent fluence correction factors h_{pl} at d_{ref} as a function of R_{50} in water for the combination of PW and PWDT phantoms and plane-parallel chambers irradiated by clinical electron beams.

565

			NACP-02		Roos	
E (MeV)	R_{50} (cm)	d_{ref} (cm)	PW	PWDT	PW	PWDT
4	1.31	0.69	1.006	1.006	0.998	0.998
6	2.37	1.32	1.001	0.998	0.996	1.001
9	3.59	2.05	1.002	1.006	0.998	0.996
12	5.06	2.94	1.001	0.997	1.003	1.000
15	6.27	3.66	0.999	0.998	1.002	1.002
18	7.60	4.46	0.998	1.003	1.002	1.005

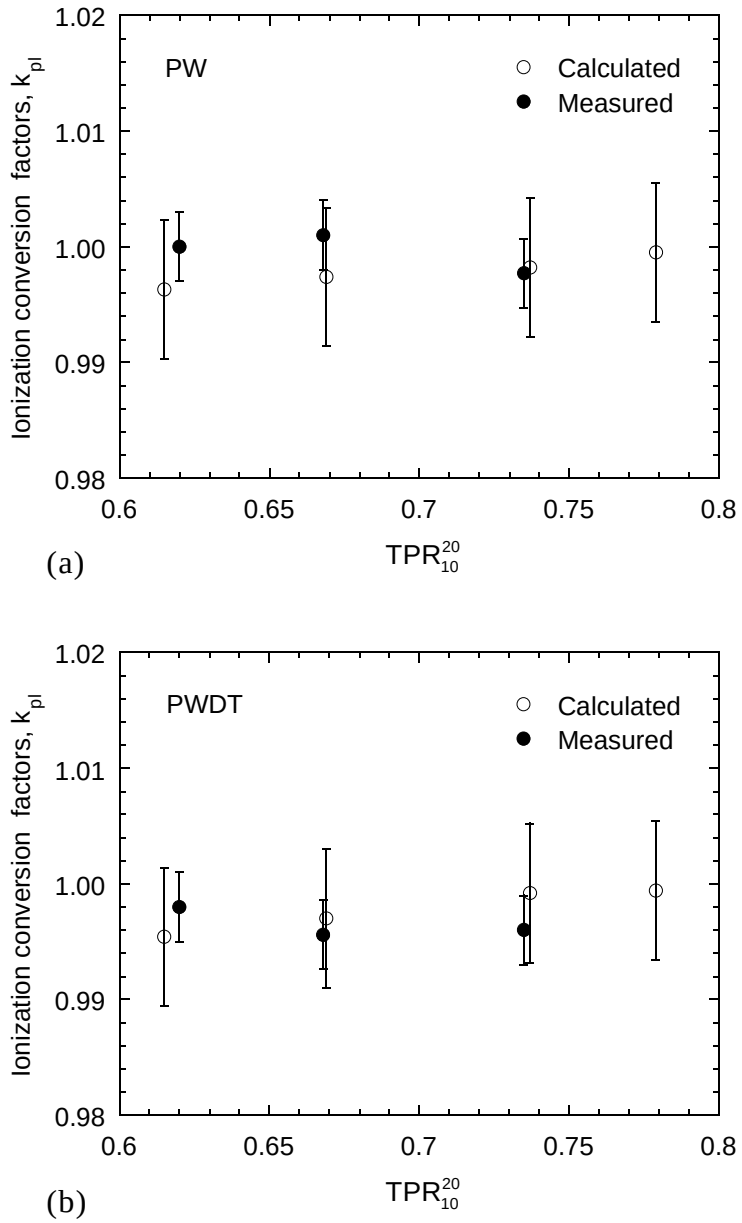

Fig. 1. Comparison of calculated and measured water-to-plastic ionization conversion factors k_{pl} at d_{ref} as a function of TPR_{10}^{20} in water for the combination of (a) PW and (b) PWDT phantoms and a PTW 30001 Farmer-type chamber irradiated by clinical photon beams at SAD=100 cm.

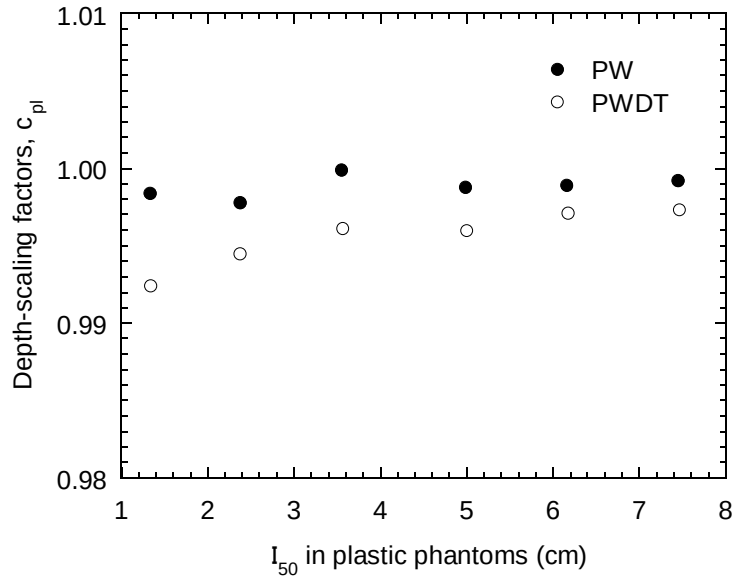

Fig. 2. Calculated depth-scaling factors c_{pl} as a function of I_{50} in PW and PWDT phantoms using clinical incident electron beams. The depth-scaling factor is calculated to ensure that the mean energies are matched at equivalent depths.

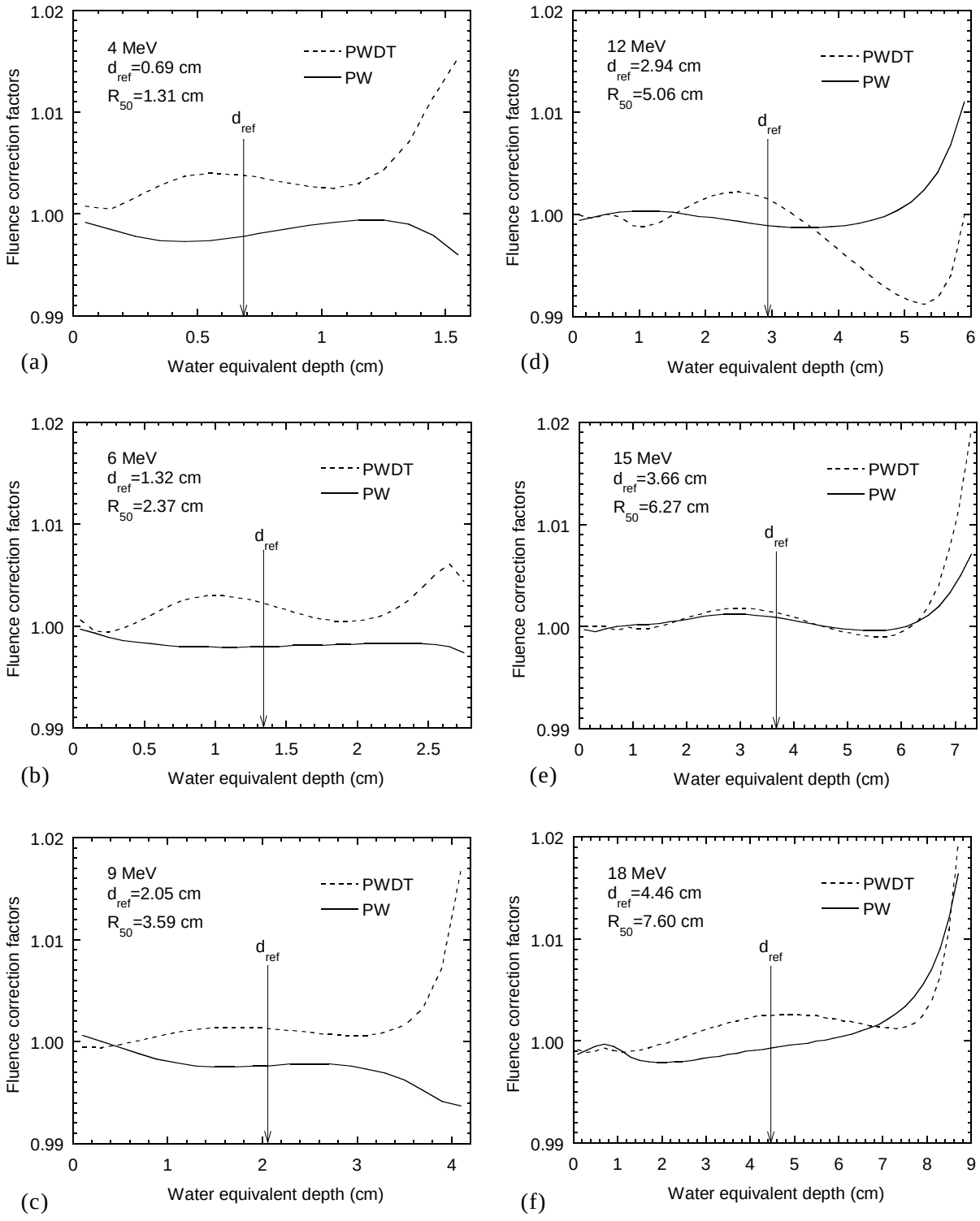

Fig. 3. Calculated fluence correction factors ϕ_{pl}^{w} as a function of water-equivalent depth in PW and PWDT phantoms for 4, 6, 12, 15, and 18 MeV electrons from Varian Clinac linear accelerators, respectively.

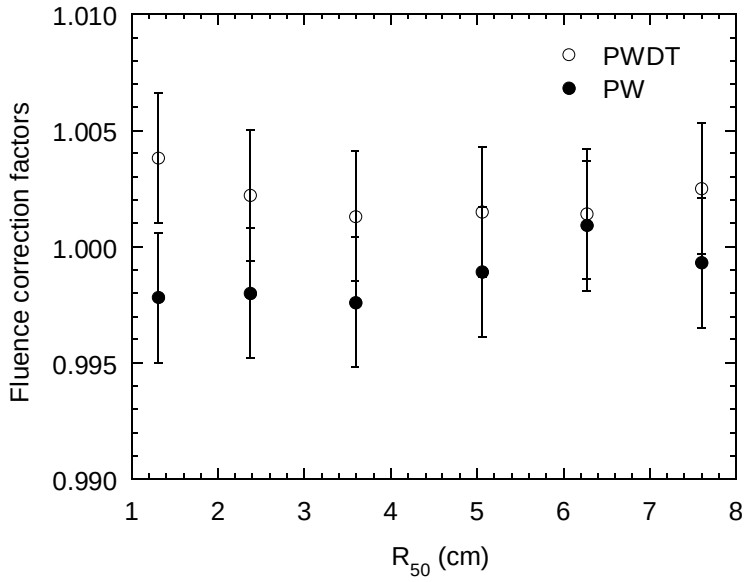

Fig. 4. Calculated fluence correction factors ϕ_{pl}^{w} at a reference depth, d_{ref}=0.6R_{50}-0.1 (cm), as a function of R_{50} in water for clinical electron beams incident on PW and PWDT phantoms.

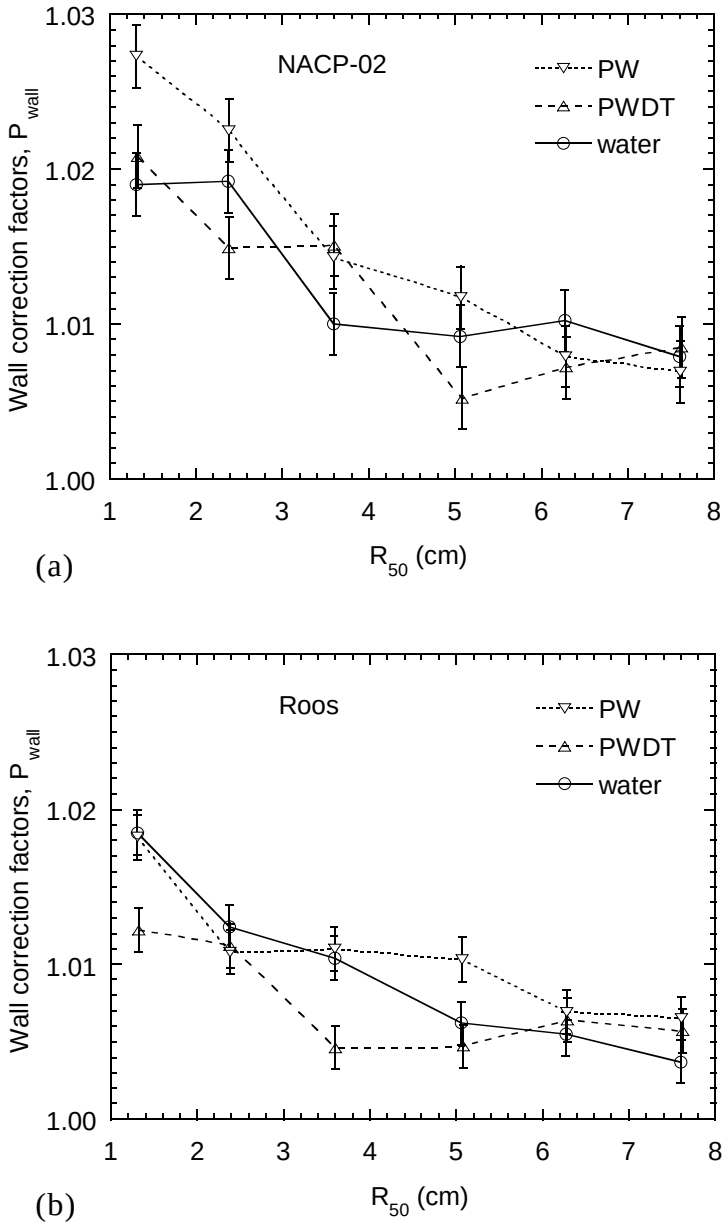

Fig. 5. Calculated wall correction factors P_{wall} at a reference depth as a function of R_{50} in water for (a) NACP-02 and (b) Roos chambers in water, PW, and PWDT phantoms irradiated by a 15×15 cm^2 beam.

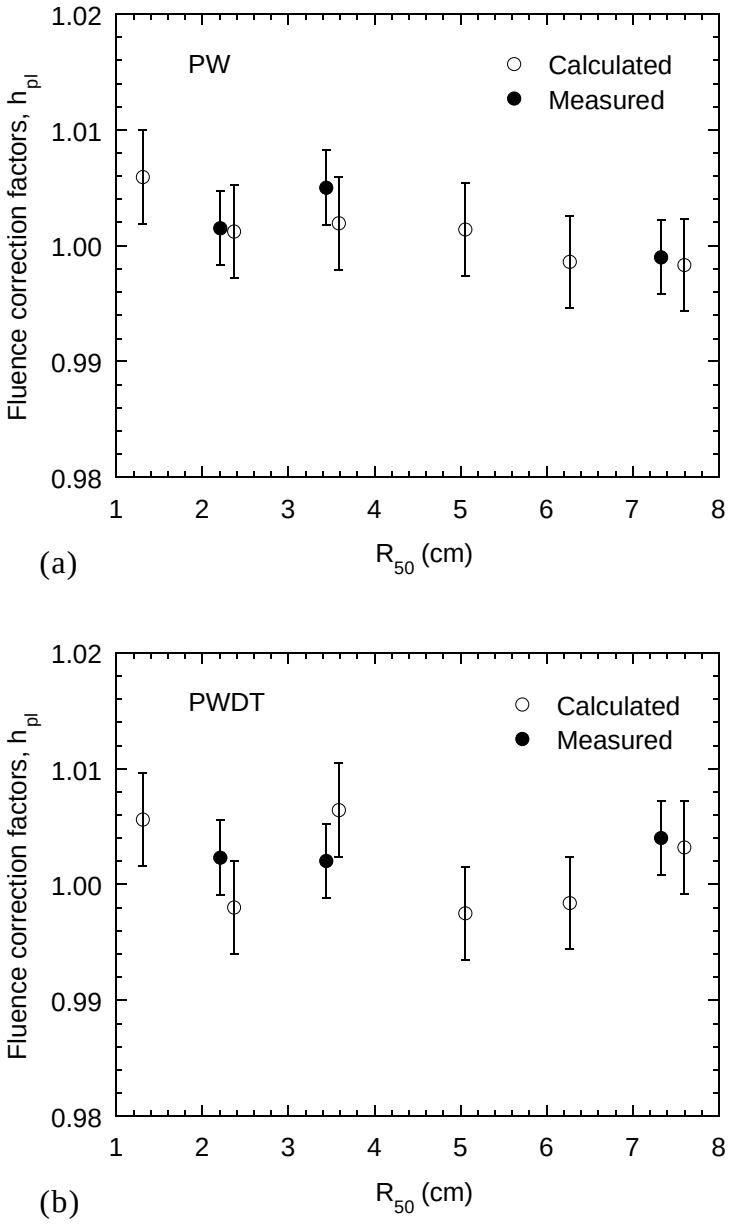

Fig. 6. Comparison of calculated and measured chamber-dependent fluence correction factors h_{pl} at d_{ref} as a function of R_{50} in water for the combination of (a) PW and (b) PWDT phantoms and an NACP-02 chamber irradiated by clinical electron beams at SSD=100 cm.